ELSEVIER

Earth and Planetary Science Letters 140 (1996) 133–146

EPSL

Astronomical calibration of the Matuyama–Brunhes boundary: Consequences for magnetic remanence acquisition in marine carbonates and the Asian loess sequences

L. Tauxe [a,b,*], T. Herbert [b], N.J. Shackleton [c], Y.S. Kok [a]

[a] *Fort Hoofddijk Paleomagnetic Laboratory, Budapestlaan 17, 3584 CD Utrecht, The Netherlands*
[b] *Scripps Institution of Oceanography La Jolla, CA 92093-0220, USA*
[c] *Godwin Institute for Quaternary Research, The Godwin Laboratory, Free School Lane, Cambridge, UK*

Received 6 September 1995; accepted 14 February 1996

Abstract

We have compiled 19 records from marine carbonate cores in which the Matuyama–Brunhes boundary (MBB) has been reasonably well constrained within the astronomically forced stratigraphic framework using oxygen isotopes. By correlation of the $\delta^{18}O$ data to a timescale based on astronomical forcing, we estimate astronomical ages for each of the MBB horizons. In all but one record the MBB occurs within Stage 19.

Most magnetostratigraphic sections in Asian Loess place the MBB within a loess interval. Since loess deposition is presumed to be associated with glacial intervals, loess horizons should correspond to even-numbered oxygen isotope stages. A glacial age for the MBB is at odds with the results presented here, which firmly place the MBB within interglacial Stage 19. Inconsistency among the many loess sections and between the loess and the marine records suggests that the magnetic interpretation of loess sections may be more complicated than hitherto supposed.

The mean of the Stage 19 age estimates for the MBB is 777.9 ± 1.8 (N = 18). Inclusion of the single Stage 20 age results in a mean of 778.8 ± 2.5 (N = 19). The astronomical age estimate of the MBB compares favorably with an (unweighted) mean of 778.2 ± 3.5 (N = 10) from a compilation of $^{40}Ar/39^{Ar}$ results of transitional lava flows. Combining the two independent data sets yields a grand mean of 778.0 ± 1.7 (N = 28).

The new compilation shows virtually no trend in placement of the MBB within isotope Stage 19 as a function of sediment accumulation rate. We interpret this to mean that the average depth of remanence acquisition is within a few centimeters of the sediment–water interface.

Separating the cores into two geographic regions (an Indo–Pacific–Caribbean [IPC] Group and an Atlantic Group) results in a significant difference in the position of the mid-point of the reversal with respect to the astronomical time scale. The data presented here suggest a difference of several thousand years between the two regions. This observation could be caused by systematic differences between the two regions in sedimentation rate within the interval of interest, systematic differences in remanence acquisition, or by genuine differences in the timing of the directional changes between the two regions.

Keywords: Matuyama Epoch; Brunhes Epoch; paleomagnetism; time scales; magnetostratigraphy; remanence magnetization; loess

* Corresponding author. E-mail: ltauxe@geof.ruu.nl

PII S0012-821X(96)00030-1

1. Introduction

The plate tectonic revolution took place in part because of technological developments in the K–Ar isotope method that allowed dating of young basalts of known magnetic polarity (see [1]). Thus was born the Geomagnetic Reversal Time Scale (GRTS) [2]. We use the term 'reversal time scale' as opposed to 'polarity time scale' because it is the reversals bracketing the polarity zones that are dated. The GRTS thus divides time into Epochs (now called Chrons) of relatively constant magnetic polarity, punctuated at apparently random intervals by reversals that have been either directly or indirectly dated.

Until recently, the last chron boundary (the Matuyama–Brunhes Boundary or MBB), was thought to have occurred some 730 thousand years ago [3], based on K–Ar data from tuffs and lava flows that bracketed the boundary (see excellent review by [4]).

Parallel to efforts at dating volcanics on land, magnetostratigraphic work in sediments placed the MBB within or near to Stage 19 in the framework of oxygen isotope variations in pelagic sediments [5]. These isotope variations reflect changes in insolation resulting from the precession and obliquity of the Earth's orbit [6,7] and have been modeled assuming various phase lags for the climatic response and details of the manner in which ice sheets grow and decay; the Ice Volume Model of, for example, [7], lags the insolation curve at 65°N by 3–4 k.y. Since orbital variations can be accurately calculated for at least the last several million years [8], the position of the MBB within the so-called Astronomical Time Scale provided independent confirmation of the 730 ka date [9]. One lone study [10] called for an older date for the MBB (790 ka), but was largely ignored.

Several developments conspired to topple the 730 ka date for the MBB. In a landmark paper, Shackleton et al. [11] suggested that the oxygen isotope records had been mismatched to the Astronomical Time Scale and that Stage 19 was actually much older; by association, the MBB was some 780 ka. Concurrently, advances in $^{40}Ar/^{39}Ar$ dating techniques vastly improved the capability of analyzing young volcanics (see summary by [4]), and the apparent discrepancy between the astronomically calibrated version of the reversal time scale and the radioisotopically calibrated reversals virtually disappeared [12–14]; indeed, some have argued that an age of 780 ka for the MBB should be taken as one of the constraints for $^{40}Ar/^{39}Ar$ calibration [15].

Despite convergence of different dating approaches on an older age for the MBB, there is still room for discussion. There is uncertainty in the exact placement of the MBB within the astronomical time scale (at the base of Stage 19 [16] or at the top [17] — a difference of some 10 k.y.). Moreover, deMenocal et al. [18] postulated that the position of the boundary may be displaced significantly downward by post-depositional processes. If this is true, then the position of the MBB within Stage 19 can only be determined using multiple cores spanning a large range of sediment accumulation rates (SARs).

In this paper, we attempt to pull together diverse evidence bearing on the age of the MBB. We examine the available oxygen isotope and lithostratigraphic records with well constrained MBBs and discuss the consequences of the compiled data set for the issue of magnetic remanence acquisition as well as the placement of the MBB within the Astronomical Time Scale. We compare the astronomically derived dates for the MBB to $^{40}Ar/^{39}Ar$ dates from volcanic units closely associated with the MBB. Finally, we discuss implications of the Stage 19 placement of the MBB for the interpretation of the magnetostratigraphies of various loess sequences in China.

2. Astronomical calibration of the MBB

DeMenocal et al. [18] compiled records from eight pelagic cores in which the MBB had been located. Seven of these had $\delta^{18}O$ data and one had a $CaCO_3$ proxy. Since then, many more records have become available and in some cases, the uncertainties in the placement of the MBB have shrunk owing to more intensive paleomagnetic sampling. One $\delta^{18}O$ record has an unacceptably large uncertainty in the placement of the MBB (more than 50 cm — DSDP Site 610) and is not used here. Moreover, the carbonate proxy record (609) has a pattern that is difficult to interpret unambiguously, and $\delta^{18}O$ data from a part of the record shows very poor agreement with the carbonate data [N. Shackleton, unpublished data]. As well as updating the compilation of deMenocal et

al., by including more recent paleomagnetic results and correcting errors in their data table, we have collected together nine records that have become available since the earlier study (marked with a + in Table 1) (from this study and [17,20,22,53–58,62–65,68]).

In addition to the new $\delta^{18}O$ records, we have four high resolution lithologic proxy records (Table 1) based on ship-board Gamma-ray Attenuation Porosity Evaluator (GRAPE) data, a good proxy for carbonate in many regions [19]. Thus, we have a total of 19 astronomically calibrated records with MBB depths ranging from 7.25 m (corresponding to an average SAR of less than 1 cm/k.y.) to depth of 64.74 m (an average SAR of about 8 cm/k.y.). Locations of the cores used in this study are shown in Fig. 1 and Table 1 [59–61,66,67].

We place the MBB at the mid-point between the lowest normally magnetized and the highest reversely magnetized specimens and the uncertainty bounds span the interval between the bracketing specimens. The MBB values for all cores whose depths have been converted to composite depths were taken from the same cores as the climatic proxy data; hence there is no additional uncertainty from core-to-core correlation of the two types of data.

The records listed in Table 1 are gleaned from literature sources with the following exceptions: Oxygen isotope data for ODP 664 are from [20]. Paleomagnetic data for ODP 552A were listed by

Table 1
Astronomical age constraints for the MBB

Core	ref.	Lat./Long.	[18.2]/18.4 (m)	MBB (m)	20.2 (m)	Age of MBB [alt.] (ka)
			Oxygen Isotopic data			
V28-239	[16]	3/159	7.10	7.25± 0.05	7.3	784.2± 9.7 [769.6]
ERDC 103p (+)	[22],this paper	-4/161	7.3	~ 7.54±.025 (cd)	7.805	769.2± 1.9
M13519 (+)	[53]	5/340	9.59	9.87± 0.015	10.02	779.1± 1.3
ODP 851E (+)	this paper,[54]	3/249	[10.75]	11.58± 0.01	11.83	774.6 ± 0.7
V28-238	[5]	1/161	11.61	12.01±.03	12.3	775.6± 1.7
ODP 758A (+)	[55, 56]	5/90	11.83	12.17± 0.05 (cd)	12.43	775.1± 9.8
ODP 805C (+)	[57, 58]	1/160	12.29	12.73 ± 0.01	13.0	777.2± 0.5
ODP 552A	[59, 21]	56/337	13.94	14.64± 0.02	14.60	796.1± 1.2
ODP 502B	[60, 61]	12/280	[15.115]	16.25± 0.05	16.64	772.8± 2.6
ODP 659A (+)	[62, 63]	18/339	21.94	22.8± 0.015	23.11	781.7± 0.5 [779.7]
ODP 664B (+)	[20, 63]	0/337	27.34	28.75± 0.015 (cd)	29.26	780.6± 0.3 [778.6]
ODP 607A	[9, 26]	41/329	30.43	31.82± 0.015 (cd)	32.32	781.7± 0.3
MD900963 (+)	[17]	5/74	33.92	35.01± 0.19	35.715	776.7± 4.1
ODP 769A (+)	[64, 65]	9/121	60.81	62.27± 0.05	63.2	776.8± 0.8
ODP 646A	[66, 67]	58/312	62.23	63.74± 0.14 (cd)	64.74	776.5± 2.2
			lithologic proxy data			
ODP 804C (+)	[58]	1/161	7.89	8.18± 0.01	8.38	776.1± 1.2
ODP 807A (+)	[68]	4/157	11.96	12.25± 0.01	12.44	776.6± 1.2
ODP 665A (+)	[63]	3/340	15.29	15.83± 0.015 (cd)	15.98	783.7 ± 0.9 [776.5]
ODP 660A (+)	[63]	10/341	18.6	19.2± 0.015 (cd)	19.37	783.5 ± 0.7
Mean of all: 778.8 ± 2.5 (N=19); excluding 552A: 777.9 ± 1.8 (N=18)						
Mean of IPC cores: 776.2 ± 2.1 (N=11); using alternate ages: 774.6 ± 1.6						
Mean Atlantic cores: 781.0 ± 1.6 (N=7); using alternate ages: 779.0 ± 1.9						

Depths are in meters below sea floor except those marked (cd), which are in composite depths. (+) were not used by [18]. Uncertainties in depths and individual age estimates reflect positions of highest (lowest) known normal (reversed) samples. Uncertainties in the means are 95% confidence in the mean ($1.96\sigma/\sqrt{N}$). Alternate ages listed in brackets are based on shifting the MBB upward by 7–10 cm, as suggested by behavior of sister cores (see text). Latitudes and longitudes are in degrees North and East, respectively.

deMenocal et al. [18] as D. Kent, unpublished. We obtained the original data [21] and the depths in Table 1 are based on those data. Paleomagnetic data for ERDC103p were first published by Tauxe and Wu [22] based on whole core measurements demagnetized in alternating fields to 15 mT. The core was subsampled and step-wise demagnetization was performed on all specimens (see examples shown in Fig. 2). On demagnetization, specimens near to the MBB that were apparently 'normal' at 15 mT, showed a small reversed characteristic component by 35 mT (see e.g. the specimen from 7.57 mbsf). Thus, the placement of the MBB 'walked up' by some 7 cm. As indicated by Tauxe and Wu [22] the top ~ 70 cm is missing from ERDC103p. The actual MBB is now placed at 6.84 ± .025 m below the top of the core; thus the MBB is estimated to be some 7.54 m below the seafloor. (N.B.: the uncertainty in the exact depth below sea floor is not reflected in the uncertainty of the relative placement of the $\delta^{18}O$ data and the MBB.)

It is also worthwhile noting here that Valet et al. [23] presented a detailed study of the MBB in ODP Holes 659C, 665B and 664D (companion holes to those with climatic proxy data used here). In all cases the MBB 'walked up' 7–10 cm upon more intensive demagnetization than the 5 mT used in ship-board measurements.

We plot our compilation of $\delta^{18}O$ data in Fig. 3. Although each is plotted against depth, the depth scales have been adjusted such that approximately the same amount of time is represented by each record. This was done by taking the depth to the MBB (shown to the right and in Table 1) and dividing by 780 k.y. (a reasonable first-order approximation for the age of the MBB), to calculate an approximate sediment accumulation rate. We plot ~ 100 k.y. on either side of the MBB. All records are plotted without a Y scale, but adjusted to have about the same amplitudes, with more negative values up, as is the convention.

Relative densities from cores with GRAPE data are plotted in Fig. 4. These are plotted in a similar manner but with a nominal 150 k.y. on either side of the MBB. We have plotted these data so as to have the sense of Stage 19 'up' in all cases, for ease of visual comparison. Thus, the density scales are opposite between the Pacific and Atlantic cores, reflecting the different paleoceanographic environments.

One goal of this study was to estimate the age of each MBB record in terms of the Astronomical Time Scale, which derives ultimately from calculations of

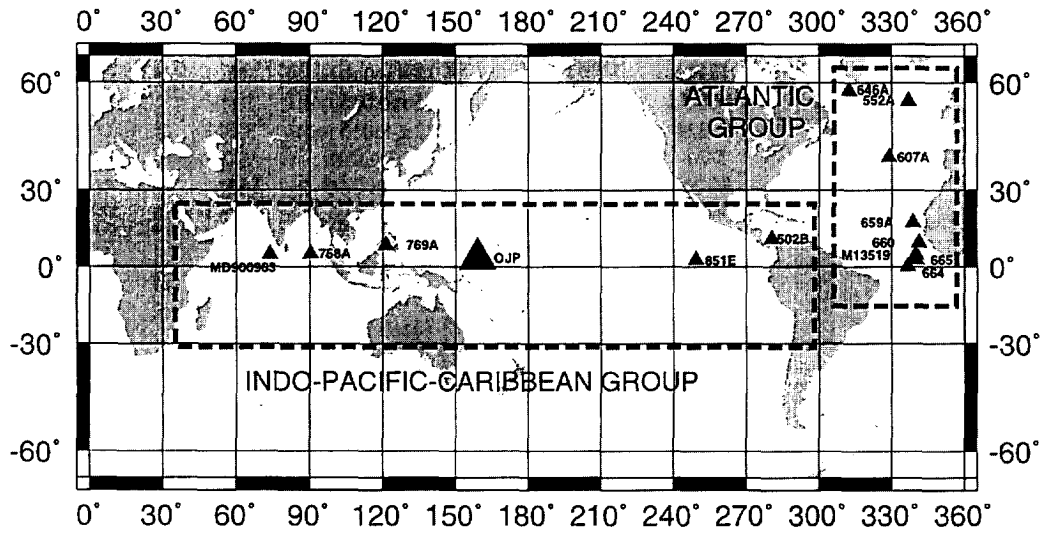

Fig. 1. Locations of cores used in this study. OJP is a cluster of cores from the Ontong–Java Plateau, including V28-238, V28-239, ERDC 103p, ODP 804C, 805C and 807A. The two geographic regions marked are the Indo–Pacific–Caribbean (IPC) Group of cores and the Atlantic Group of cores.

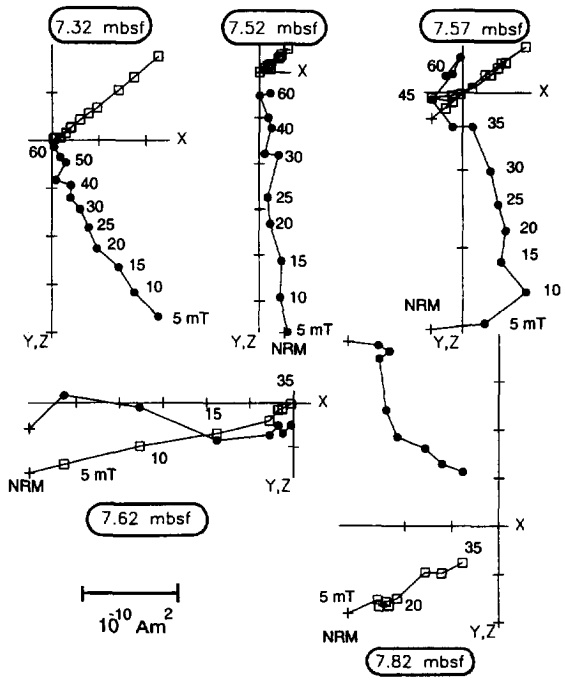

Fig. 2. Representative demagnetization data from ERDC103p. Depths are in meters below the sea floor and have been adjusted by 0.7 m from the core top. Plots are orthogonal projections with solid symbols begin on the horizontal plane and open symbols on the X,Z plane. The demagnetization was by alternating fields, at 5 mT intervals.

insolation variations occurring from peculiarities of the Earth's orbit. These calculations are thought to be robust for at least the last 3 million years [8]. The theory that oxygen isotopes are forced by these orbital parameters is well established [6] and the time lags built into models of ice volume changes resulting from the changes in insolation are reasonably well known [7] and, in any case, are rather small (a few thousand years) compared to uncertainties resulting from sampling density and analytical problems. In fact, competing climatic models (e.g. [24] and [7]) differ by only a few thousand years. Thus, the uncertainty contributable to unknown phase lags is of the order of the uncertainty in boundary placement.

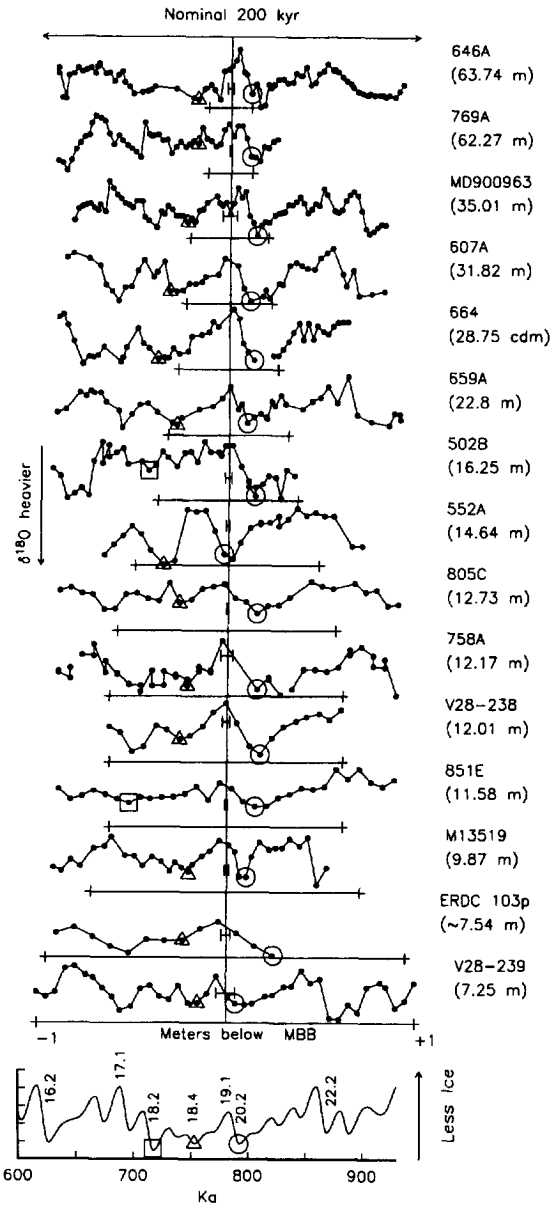

Fig. 3. (a) Summary of oxygen isotope records containing well defined Matuyama Brunhes boundaries (MBBs). See Table 1. Each record is centered on the position of the MBB (the long vertical line) and the uncertainty of this position is indicated by the small error bars about the vertical line. In certain cores, the uncertainties are smaller than the thickness of the vertical line and do not appear. Meter levels above (−1) and below (1) the MBB are indicated by the heavy horizontal line below each record. The records are plotted to represent a nominal 200 ka about the boundary (see text). Open symbols indicate our correlation tie points of the oxygen isotope records to the 'Ice Volume' Model [7] forced by the orbital insolation variations of [8]. The stage terminology (e.g. 18.2) is after [25]. See Table 1 and text for data sources.

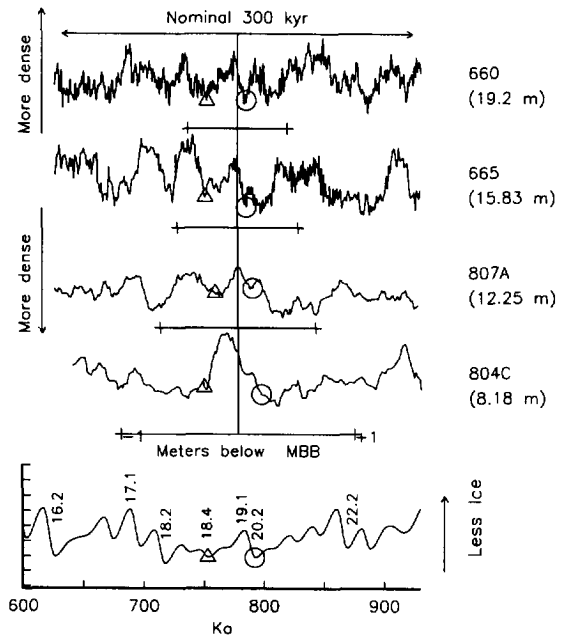

Fig. 4. GRAPE records containing well defined MBB (see text, Table 1 and caption of Fig. 3).

As a means of tying the $\delta^{18}O$ records to the Astronomical Time Scale, we use the Ice Volume Model of Imbrie and Imbrie [7] forced by the orbital insolation; variations of [8] (plotted at the bottom of Fig. 3). For convenience, we have labelled several features in the Ice Volume Model according to the nomenclature of Prell et al. [25].

Assuming that our initial guesses about average SARs are approximately correct, each $\delta^{18}O$ record should span from approximately 680 ka (or about Stage 17) to 880 ka (or around Stage 22/23). Further, assuming that the MBB falls near or in Stage 19 [5,16,9,17], we pick several points for each record which tie it to the Ice Volume Model as shown in Fig. 3.

Uncertainty in the placement of the MBB results partly from sampling density, but also from the facts that:

1. the transition takes a finite amount of time at a given location (as much as 5000 yr, based on the highest resolution sedimentary records, (e.g. [26]);
2. the transition is associated with low paleointensities and sediments retain a dramatically poorer

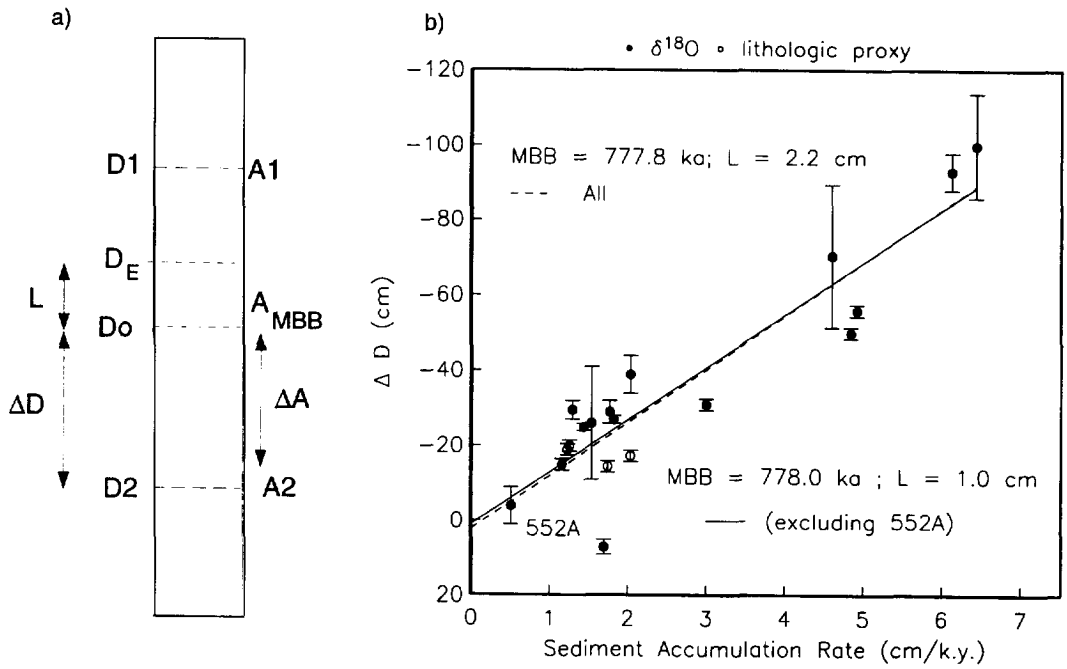

Fig. 5. (a) Some definitions used in this paper. (b) ΔD plotted against Sediment Accumulation Rate. Short dashed line is the regression for the entire data set. The solid line is the regression excluding Site 552A.

record of the field during the transition than outside of it (see, e.g., [17,26] for details);

3. magnetic overprinting affects low intensity sediments more strongly [27];
4. [24] and [29] documented a global dip in paleointensity preceding the MBB by some 15 k.y. that is sometimes accompanied by normal polarity directions. These normal directions usually, but not always, disappear on demagnetization. In cases of inadequate sampling, there is the danger of misidentifying this so-called 'Brunhes-precursor' as the MBB itself. It is therefore possible that the reported MBB at Site 552A (the only one to occur in Stage 20) has been so misidentified. The 50 cm interval immediately overlying the presumed boundary suffers from severe coring disturbance, hence it is not possible to test whether the 'real' MBB lies some 25 cm above that currently identified. We therefore treat this record with some caution in the section on data analysis.

Oxygen isotope data can be noisy and are often sampled at relatively large intervals. Estimation of sediment densities using a GRAPE recorder aboard ships of the Deep Sea Drilling Project (DSDP) and the Ocean Drilling Program (ODP) are often less noisy and are made at closer intervals. While the interpretation of GRAPE data in terms of paleoclimatic significance is not without problems, GRAPE data can be correlated to $\delta^{18}O$ data with a high degree of success in several regions. (The phase of the Pacific and Atlantic sites is, however, different by 180°.) We therefore supplement our $\delta^{18}O$ data set using GRAPE data from four cores in which the phase relations between GRAPE and $\delta^{18}O$ have been firmly established. These data are shown in Fig. 4.

DeMenocal et al. [18] found that the data they examined showed a dependency of the location of the MBB within Stage 19 on sediment accumulation rate. The boundary was apparently shifted down in cores with slower sediment accumulation rates. They interpreted their data (after adjusting with an assumed mixing model) to mean that the paleomagnetic signal is fixed some 16 cm below the sediment–water interface.

The problem described here is one in which two temporally discrete events are recorded in sediments (Fig. 5a). We suppose that one of the events is recorded at some depth, L, below the sediment–water interface. If the sediment accumulation rate (SAR) is known, then both L and the age difference between the two events (ΔA) can be determined by linear regression (see [30]).

From the data in Table 1, we know the depths of two isotope tie points whose ages were determined by correlation to the Ice Volume Model (see Figs. 3 and 4). We use isotope Stage 18.2 (717 ka) or 18.4 (753 ka) and 20.2 (792 ka). The sediment accumulation rate for each core in the interval associated with the MBB is:

$$\mathrm{SAR} = \frac{D_2 - D_1}{A_2 - A_1}$$

where the ages (A_i) and depths (D_i) are those of the two tie points. Neglecting L for the moment, we can estimate an astronomical age (A_{MBB}) for the depth of the MBB (D_o) in each core by interpolation:

$$A_{\mathrm{MBB}} = [D_o - D_1]/\mathrm{SAR} + A_1$$

The individual age estimates for the MBB are listed in Table 1, along with the uncertainties derived from the uncertainty in placement of the MBB. One should be aware however, that there is also an unknown contribution to the uncertainty in A_{MBB} by variations in SAR between the two tie points. The mean of the astronomical estimates for the MBB is 778.8 ± 2.5 (N = 19), or 777.9 ± 1.8 ka (N = 18) excluding Site 552A.

Based on our experience with ERDC 103p, we believe it possible for the MBB in a neighboring core, V28-239, to also suffer from overprinting. V28-239 was only lightly demagnetized (5 mT), and has one of the lowest occurrences of the MBB with respect to the isotope record (an estimated age of 784.2 ± 9.7). If the MBB in V28-239 were to 'walk up' some 7 cm, as it did in the sister core ERDC 103p, the age estimate for the MBB would be 769.6 ka. Similarly, if the MBBs in 656A, 664B, and 665A are also displaced upwards by 10 cm, consistent with the data of [23], the ages would be 779.7, 778.6, and 776.5 ka, respectively. These alternative ages for the MBBs are listed in brackets in Table 1. The mean calculated using the alternative MBB placements (and excluding 552A) is 776.7 ± 1.7, suggesting that problems with overprinting do not seriously affect the estimate in the age of the MBB.

The expected depth of the MBB (D_E) depends on SAR and the assumed age of the MBB ($\bar{A}$). Taking ΔA as $\bar{A} - A_2$, we have:

$$D_E = \Delta A \cdot \mathrm{SAR} + D_2$$

The observed depth D_o is D_E plus some offset, L, so:

$$D_o = \Delta A \cdot \mathrm{SAR} + D_2 + L$$

Taking $\Delta D = D_o - D_2$ we have:

$$\Delta D = \Delta A \cdot \mathrm{SAR} + L$$

Thus, both the so-called 'lock-in depth', L, and an estimate for the age, $\bar{A}$, can be obtained by linear regression.

We plot ΔD versus SAR for all the cores in Table 1 in Fig. 5b. Regression of the entire data set yielded $L = 2.2$ cm and $\bar{A} = 777.8$ ka. Regression of the data set excluding Site 552A yielded $L = 1.0$ cm and $\bar{A} = 778.0$ ka. (Exclusion of V28-239 yielded virtually identical results). These age estimates for the MBB are indistinguishable from the mean of those estimates made by neglecting L, in an *a posteriori* justification of the approach.

Thus, given the reasonable grounds for suspecting Site 552A to be in error, we view a depth offset of a few centimeters to be a conservative estimate for the average depth at which sediments are magnetized. This analysis differs from that of deMenocal et al., who found $L \sim 16$ cm based on a smaller and less well constrained data set.

3. Discussion

3.1. Implications for the interpretation of Asian loess sequences

Climatic variations due to changes in insolation are recorded not only in the oceans, but also in continental sequences. In particular, the great Asian loess sequences appear to retain a remarkable sequence, reflecting the changing climate in the loess/paleosol record (see [31] for an excellent review). Loess, composed of dust ground by glaciers, is assumed to accumulate more rapidly during the colder, drier periods associated with greater glacial activity (the even-numbered isotope stages). Paleosols and weathering horizons are assumed to form during the warmer, wetter interglacials (odd isotopic stages), thus suggesting the possibility of a rare, high-resolution correlation between continental and marine sequences (see [32–34]).

Since the MBB is firmly tied to Stage 19, a period of less ice, it should be found in a paleosol horizon in the continental sequences. While this was the case in some studies from the Luochan area in China (paleosol S8: [35–37]), others appear to place the boundary within the overlying loess horizon (L8) [38]. However, Hus and Han [39] sampled L8 at Luochan in great detail and found the entire interval to be uniformly normally magnetized. All other studies from Asian loess sections seem to place the boundary within a loess interval (e.g., Xifeng: [38,40,41], Lanzou: [42,43], Baoji: [44,32], Karamaidan: [34], and Weinan [45]).

Several authors have attempted to correlate the loess stratigraphy with the δ^{18}O record. Ding et al. [33] compared the grain size stratigraphy from the Baoji loess sequence with the δ^{18}O SPECMAP stack [46] and Rutter et al. [32] compared the loess/paleosol sequences at Baoji with the oxygen isotopic stack of Williams et al. [47]. Forster and Heller [34] compared susceptibility logs from the Karamaidan and Xifeng sections to the δ^{18}O record from ODP 677 of [11]. The consensus seems to be that there is a firm correlation between the continental and marine sequences (see, e.g., [31]), while, in fact, the placement of the MBB in the two is apparently discrepant. Interestingly, the specific location of the MBB within the various δ^{18}O timescales used contributed to the perception that the correlation was straightforward. The MBB in the SPECMAP stack was based largely on V28-239, a core in which the MBB is among the lowest in our collection. The SPECMAP timescale was shown to be in error by Shackleton et al. [11], based on the δ^{18}O record of ODP 677, a core with no magnetostratigraphy. Finally, the timescale of Williams et al. [47] was based on DSDP 504 (no paleomagnetic data), V28-239 (MBB lower than average), DSDP 552A (MBB almost certainly too low) and DSDP 502B. Based on these records, Rutter et al. [32] incorrectly assumed that the MBB was in Stage 20. While [34] were concerned with what appeared to be a slight offset from the base of Stage 19 to mid-Stage 20, we find here that the discrepancy is actually much worse

than previously imagined. Forster and Heller [34] considered the following possible causes for the offset: (1) phase lags between the continental and oceanic responses, and (2) differential 'lock-in' depth. They cited the deMenocal et al. [18] finding that the placement of the MBB in deep-sea sediments was a strong function of sediment accumulation rate, a finding we revise. They further pointed out that the MBB in closely spaced loess sequences in the Luochan area is not strictly synchronous [48], but varies in placement within paleosol S8. Furthermore, as already noted, many loess sequences show the MBB within a loess. Finally, most records appear to be severely overprinted (e.g. [43]) and studies attempting to investigate high resolution 'geomagnetic field behavior' in loess sequences (e.g. [41]) display highly complex remanence characteristics similar to those found in red bed paleosols [49].

Because of the high degree of variability in placement of the MBB within the loess sequences, the complex magnetic mineralogy and the evidence for severe overprinting, we favor some form of 'delayed remanence acquisition' in the loess sequences as opposed to a phase lag between oceans and continents. Also, if the remanence has been so severely altered, the question arises as to what effect the pervasive secondary alteration has on the bulk magnetic properties and the correlation of magnetic susceptibility with the $\delta^{18}O$ records. In fact, it is quite plausible that L8 corresponds to Stage 20, on the basis that overprinting generally shifts normal boundaries downward; hence, S7, not S8, may correspond to Stage 19.

3.2. Depth of remanence acquisition

The sediment–water interface is subject to a variety of processes including bioturbation, diagenesis, and physical erosion. It would be astounding if a single depth existed at which magnetic remanence was acquired, regardless of large variations in environmental factors such as SAR, carbonate percentage, surface productivity, chemistry of the sediment–water interface, and grain size. Such vari-

Table 2
$^{40}Ar/^{39}Ar$ ages constraining the age of the MBB

Unit #	Location	Polarity	Age (ka)	Ref.
1	Silbo, Kenya	Normal	740 ± 10	[69]
2	Olorgasaile, Kenya	Normal	746 ± 9	[12]
3	Bishop Tuff, CA	Normal	757 ± 9	[4]
4	Bishop Tuff, CA	Normal	764 ± 5	[4]
5	Volcán Tatara-San Pedro, Chile	Normal	765.2 ± 7.5	[52]
6	Volcán Tatara-San Pedro, Chile	Normal	767.2 ±15	[52]
7	Maui, Hawaii	Transitional	770.8 ± 5.5	[52]
8	Maui, Hawaii	Transitional	770.8 ± 5.2	[52]
9	Maui, Hawaii	Transitional	772 ± 14	[13]
10	La Palma, Canary Islands	Transitional	774.6 ± 14	[52]
11	Volcán Tatara-San Pedro, Chile	Transitional	778.4 ±6.3	[52]
12	Maui, Hawaii	Transitional	780 ± 10	[13]
13	Volcán Tatara-San Pedro, Chile	Transitional	780.5 ±3.7	[52]
14	Volcán Tatara-San Pedro, Chile	Transitional	783.0±3.5	[52]
15	Tahiti	Transitional	784.6 ± 7.1	[52]
16	Maui, Hawaii	Transitional	787 ± 12	[13]
17	Oldest Toba Tuff, Sumatra	Reversed	789 ± 6	[4]
18	Valles Caldera, NM	Reversed	794 ± 7	[4]
19	758A tephra , Indian Ocean	Reversed	800 ± 19.9	[56]
Mean of transitional $^{40}Ar/^{39}Ar$ data: 778.2 ± 3.5 (N=10)				

Data from [4,12,13,52,56,69].

ability in remanence acquisition is, indeed, reflected in the scatter in ΔD (see Fig. 5b) about the best-fit line. Of course, an unknown amount of the scatter is caused by variation in SAR between the two tie points; thus the scatter in ΔD is a maximum estimate for the variability in depth at which remanence is acquired. Nonetheless, the shift away from the best-fit line offers little justification for a very long delay in remanence acquisition in most marine carbonates. Indeed, the average depth of remanence acquisition appears to be within a few centimeters of the sediment–water interface.

Several other lines of evidence support the contention that remanence is acquired within a few centimeters of the sediment–water interface, as opposed to much deeper (8–16 cm), as popularly believed [50]. First, we would expect that relative paleointensity derived from sediments would be constant over the mixed layer, then begin to change, reflecting some smoothed version of changes in geomagnetic field intensity. In a study of box cores from the Ontong–Java Plateau [51], we found that the relative intensities were indeed constant over the top 3 cm, then varied according to the geomagnetic field below that. Secondly, [29] found that relative paleointensity records from pelagic carbonate sequences of a 40 k.y. period spanning the MBB, from cores with SARs ranging from 1 to 11 cm/k.y., preserved the same general features (in particular, a low intensity interval some 15 k.y. prior to the MBB). These data support a thin zone of remanence acquisition, because smoothing over a large interval would tend to smear out features in the record such as the Brunhes pre-cursor in the low SAR cores (as argued by [28]). Finally, the most carefully supported argument for remanence acquisition at depth is that of [18]; we have shown here that their conclusion is no longer supportable.

3.3. $^{40}Ar/^{39}Ar$ results and the MBB

In Table 2, we summarize $^{40}Ar/^{39}Ar$ data from volcanic units spanning the MBB with analytical uncertainties < 20 ka. In a recent compilation of $^{40}Ar/^{39}Ar$ data [52], Singer and Pringle calculated a weighted mean of their data to be 778.9 ± 1.8 ka. Weighting data by the analytical uncertainty assumes that all the uncertainty is reflected in the quoted analytical uncertainties. This may not be the case, because ages derived from plateaus sometimes differ from isochron ages from the same samples by more than the quoted analytical uncertainties. We prefer to use an unweighted mean and the 95% confidence in the mean as the uncertainty. Using only data with analytical uncertainties < 20 ka and the 95% confidence limits of $1.96\sigma/\sqrt{N}$, we calculate a mean of data from transitional lava flows of 778.2 ± 3.5 ka, which is indistinguishable from the mean of the astronomical ages.

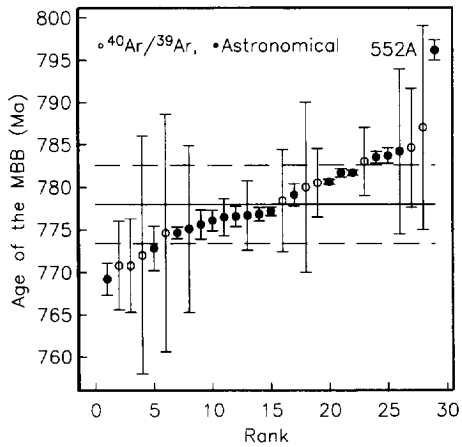

Fig. 6. Compilation of all ages for the MBB plotted according to rank (see Table 1 and Table 2). Solid line is the mean (excluding 552A) and the dashed lines are 1σ bounds.

We plot the $^{40}Ar/^{39}Ar$ data together with the astronomical age estimates in Fig. 6. These have been sorted and are plotted versus rank. Also shown are the grand mean (excluding the outlier 552A) and the 1σ bounds of the combined data set. The two data sets appear to be compatible.

Based on their statistical analysis of the data, Singer and Pringle suggested that there is a detectable difference in transitional ages between Hawaii and Chile, and argue that the directional changes at the MBB lasted some 12 ± 6 k.y. It is well documented in detailed sedimentary records that the reduction in paleointensity associated with the MBB lasted some 10 k.y (see [29] for a recent compilation), whereas the duration of directional change at a single location is at most half that (see [26]). From the point of view of magnetohydrodynamic models of reversals, it is certainly possible, if

not likely, that transitional directions could be seen at different times in different locations during the overall period of low dipole intensity (C. Constable, pers. commun.). Such diachronism would be observed here as a geographical trend in the position of the MBB with respect to the climatic template (which is likely to be isochronous around the globe). Thus, given the relatively broad global coverage of the records compiled here, it is worth examining the data for regional groupings of age estimates.

Considering the data in Table 1 and Fig. 1, it does appear that the cores from the Indian and Pacific Oceans, and the Caribbean Sea (the Indo–Pacific–Caribbean or IPC Group in Fig. 1) are systematically younger than the Atlantic Group cores. The IPC group have a mean of 776 ± 2 ($N = 11$) as opposed to 781 ± 2 ($N = 7$) for the Atlantic Group (excluding 552A).

It is possible to suggest that the 'age' difference between the Atlantic and IPC Groups of cores is the result of 'delayed acquisition' of remanence in the Atlantic set relative to the Pacific set. As previously mentioned, it is likely that the V28-239, 659, 664 and 665 age estimates are somewhat too old. Using the alternative ages listed in Table 1 the IPC set has a mean of 774.6 ± 1.6 ($N = 11$) and the Atlantic (excluding 552A) has a mean of 779.0 ± 1.9; these are still significantly different. Furthermore, the assumption that the age offset in the Atlantic cores is the result of delayed acquisition, requires that the MBB in core 607A be too low by some 25 cm, an offset hard to reconcile with the data presented by [26]. Finally, it seems to us that the Pacific group cores would be equally susceptible to overprinting (and we have argued the case for V28-239). It is also possible to explain the apparent age discrepancy between the IPC and the Atlantic cores by calling on systematic changes in sediment accumulation rate between the two tie points used. Such subtle changes are beyond the resolution of the current data set to detect.

At face value, our data appear to suggest a difference of at least several thousand years in the timing of the mid-point of the transition in the different regions, in accord with the lower bounds of the Singer and Pringle estimate. Our data therefore are consistent with the following observations: (1) the transitional depression in global dipole moment probably lasts some 10 k.y. [29]; (2) the actual change from southerly to northerly directions may occur at different times in different places (our data support a time difference of several thousand years between the IPC and the Atlantic regions); (3) transitional directions are observed over an interval of at most 5 kyr in any one place [26].

4. Conclusions

Based on the data drawn together here we conclude:

1. The magnetostratigraphic correlations between the Asian loess sequences and the $\delta^{18}O$ time scales are more complicated than previously realized.
2. The astronomical age of the MBB is some 778 ± 2 ka which compares well with the age of 778 ± 4 ka obtained from $^{40}Ar/^{39}Ar$ results from transitional lava flows. The combined data set of astronomical (excluding one outlier) and the $^{40}Ar/^{39}Ar$ data gives a grand mean of 778 ± 2 ($N = 28$). This is currently the best estimate for the MBB available.
3. Magnetic remanence in pelagic carbonates is acquired at variable depths, but on average, it is fixed within a few centimeters of the sediment–water interface.There appears to be a systematic difference in the placement of the MBB with respect to the oxygen isotope records, with Indo–Pacific–Caribbean cores appearing to be slightly younger (some 775 ± 2) than the Atlantic cores (some 781 ± 2) suggesting a diachronous occurrence of the directional changes occurring within the overall (probably synchronous) low intensity period associated with the geomagnetic reversal. Alternative explanations for the apparent age discrepancy between the two regions include systematic differences in sedimentation rates and/or 'delayed acquisition' of remanence in the Atlantic relative to the Pacific cores.

Acknowledgements

We acknowledge B. Singer and M. Pringle for access to a preprint of their manuscript. Thanks are also due to D. Kent and M. Raymo for unpublished

data. The manuscript was improved by reviews of P. Renne, B. Singer, and C. Laj. We thank Simon Crowhurst for editorial help. We also thank W. Berger, C. Constable, C. Langereis, J. Gee, P. Hartl, T. Pick, and M. Yasuda for stimulating and useful conversations. This work was supported in part by NSF Grant EAR93-15628 and a grant from GOA. The first author acknowledges partial support from Utrecht University. *[RV]*

References

[1] W. Glen, The Road to Jaramillo, Stanford University Press, 1982.

[2] A. Cox, R. Doell and G. Dalrymple, Reversals of the Earth's magnetic field, Science 144, 1537–1543, 1964.

[3] E. Mankinen and G. Dalrymple, Revised geomagnetic polarity time scale for the interval 0–5 m.y. B.P., J. Geophys. Res. 84, 615–626, 1979.

[4] G. Izett and J. Obradovitch, $^{40}Ar/^{39}Ar$ age constraints for the Jaramillo normal subchron and the Matuyama–Brunhes geomagnetic boundary, J. Geophys. Res. 99, 2925–2934, 1994.

[5] N. Shackleton and N. Opdyke, Oxygen isotope and paleomagnetic stratigraphy of equatorial Pacific core V28-238: oxygen isotope temperatures and ice volumes on a 10^5 year and 10^6 year scale, Quat. Res. 3, 39–55, 1973.

[6] J. Hays, J. Imbrie and N. Shackleton, Variations in the Earth's orbit: pacemaker of the ice ages, Science 194, 1121–1132, 1976.

[7] J. Imbrie and J. Imbrie, Modeling the climatic response to orbital variations, Science 207, 943–953, 1980.

[8] A. Berger and M. Loutre, Astronomical solutions for paleoclimate studies over the last 3 million years, Earth Planet. Sci. Lett. 111, 369–382, 1992.

[9] W. Ruddiman, M. Raymo, D. Martinson, B. Clement and J. Backman, Pleistocene evolution: Northern hemisphere ice sheets and North Atlantic Ocean, Paleoceanography 4, 353–412, 1989.

[10] R. Johnson, Brunhes–Matuyama magnetic reversal dated at 790,000 yr BP by marine-astronomical correlations, Quat. Res. 17, 135–147, 1982.

[11] N. Shackleton, A. Berger and W. Peltier, An alternative astronomical calibration of the lower Pleistocene timescale based on ODP Site 677, Trans. R. Soc. Edinburgh: Earth Sciences 81, 251–261, 1990.

[12] L. Tauxe, A. Deino, R. Potts and A. Behrensmeyer, Pinning down the Brunhes/Matuyama and upper Jaramillo boundaries: a reconciliation of orbital and isotopic time scales, Earth Planet. Sci. Lett. 109, 561–572, 1992.

[13] A. Baksi, V. Hsu, M. McWilliams and E. Farrar, $^{40}Ar/^{39}Ar$ dating of the Brunhes–Matuyama geomagnetic field reversal, Science 256, 356–357, 1992.

[14] T. Spell and I. McDougall, Revisions to the age of the Brunhes–Matuyama boundary and the Pleistocene geomagnetic polarity time scale, Geophys. Res. Lett. 19, 1181–1184, 1992.

[15] P. Renne, A. Deino, R. Walter, B. Turrin, I. Swisher, C.C.T. Becker, G. Curtis, W. Sharp and A.-R. Jaouni, Intercalibration of astronomical and radioisotopic time, Geology 22, 783–786, 1994.

[16] N. Shackleton and N. Opdyke, Oxygen isotope and paleomagnetic stratigraphy of Pacific core V28-239 Late Pliocene to Latest Pliocene, in: Investigations of Late Quaternary Paleoceanography and Paleoclimatology, R. Cline and J. Hays, eds., Geol. Soc. Am. Mem. 145, 449–464, 1976.

[17] F. Bassinot, L. Labeyrie, E. Vincent, X. Quidelleur, N. Shackleton and Y. Lancelot, The astronomical theory of climate and the age of the Brunhes–Matuyama magnetic reversal, Earth Planet. Sci. Lett. 126, 91–108, 1994.

[18] P. deMenocal, W. Ruddiman and D. Kent, Depth of p-DRM acquisition in deep-sea sediments — a case study of the B/M reversal and oxygen isotopic stage 19.1, Earth Planet. Sci. Lett. 99, 1–13, 1990.

[19] T. Herbert and L. Meyer, Long climatic time series from sediment physical property measurements, J. Sed. Petrol. 61, 1089–1100, 1991.

[20] M. Raymo, unpublished data, 1996, personal communication.

[21] D. Kent, unpublished data, 1996, personal communication.

[22] L. Tauxe and G. Wu, Normalized remanence in sediments of the Western Equatorial Pacific, relative paleointensity of the geomagnetic field?, J. Geophys. Res. 95, 12,337–12,350, 1990.

[23] J. Valet, L. Tauxe and B. Clement, Equatorial and mid-latitude records of the last geomagnetic reversal from the Atlantic Ocean, Earth Planet. Sci. Lett. 94, 371–384, 1989.

[24] W.H. Berger, T. Bickert, G. Wefer and M.K. Yasuda, Brunhes–Matuyama boundary: 790 k.y. date consistent with ODP Leg 130 oxygen isotope records based on fit to Milankovitch template, Geophys. Res. Lett. 22, 1525–1528, 1995.

[25] W. Prell, J. Imbrie, D. Martinson, J. Morely, N. Pisias, N. Shackleton and H. Streeter, Graphic correlation of oxygen isotope stratigraphy application to the Late Quaternary, Paleoceanography 1, 137–162, 1986.

[26] B. Clement and D. Kent, Geomagnetic polarity transition records from five hydraulic piston core sites in the North Atlantic, Init. Rept. DSDP 94, 831–852, 1986.

[27] Y. Gallet, J. Gee, L. Tauxe and J. Tarduno, Paleomagnetic analyses of short normal polarity magnetic anomalies in the Matuyama Chron, Proc. ODP Sci. Results 130, 547–559, 1993.

[28] D. Kent and D. Schneider, Correlation of paleointensity records in the Brunhes/Matuyama polarity transition interval, Earth Planet. Sci. Lett. 129, 135–144, 1995.

[29] P. Hartl and L. Tauxe, A precursor to the Matuyama/Brunhes transition — field instability as recorded in pelagic sediments, Earth Planet. Sci. Lett., in press.

[30] C. Burns, Timing between a large impact and a geomagnetic reversal and the depth of NRM acquisition in deep sea

sediments, in: Geomagnetism and Paleomagnetism, F.E.A. Lowes, ed., pp. 253–261, 1989.
[31] F. Heller and M.E. Evans, Loess magnetism, Rev. Geophys. 33, 211–240, 1995.
[32] N. Rutter, Z. Ding and T. Liu, Comparison of isotope stages 1-61 with the Baoji-type pedostratigraphic section of north-central China, Can. J. Earth Sci. 28, 985–990, 1991.
[33] Z. Ding, Z. Yu, N.W. Rutter and T. Liu, Towards an orbital time scale for Chinese Loess deposits, Quat. Sci. Rev. 13, 39–70, 1994.
[34] T. Forster and F. Heller, Loess deposis from the Tajik depression (Central Asia): magnetic properties and paleoclimate, Earth Planet. Sci. Lett. 128, 501–512, 1994.
[35] F. Heller and T. Liu, Magnetostratigraphical dating of loess deposits in China, Nature 300, 431–433, 1982.
[36] F. Heller and T. Liu, Magnetism of Chinese loess deposits, Geophys. J. R. Astron. Soc. 77, 125–141, 1984.
[37] F. Heller and T. Liu, Paleoclimatic and sedimentary history from magnetic susceptibility of loess in China, Geophys. Res. Lett. 13, 1169–1172, 1986.
[38] G. Kukla and Z. An, Loess stratigraphy in central China, Paleogeogr. Paleoclimat. Plaeoecol. 72, 203–225, 1989.
[39] J. Hus and J. Han, The contribution of loess magnetism in China to the retrieval of past global changes — some problems, Phys. Earth Planet. Sci. Lett. 70, 154–168, 1992.
[40] X. Liu, T. Liu, T. Xu, C. Liu and M. Chen, The Chinese loess in Xifeng, I. The primary study on magnetostratigraphy of a loess profile in Xifeng area, Gansu province, Geophys. J. 92, 345–348, 1988.
[41] D. Sun, J. Shaw, Z. An and T. Rolph, Matuyama/Brunhes (M/B) transition recorded in Chinese Loess, J. Geomagn. Geoelectr. 45, 319–330, 1993.
[42] D.W. Burbank and J. Li, Age and paleoclimatic significance of the loess of Lanzhou, North China, Nature 316, 429–431, 1985.
[43] T.C. Rolph, J. Shaw, E. Derbyshire and J. Wang, A detailed geomagnetic record from Chinese loess, Phys. Earth Planet. Inter. 56, 151–164, 1989.
[44] N. Rutter, Z. Ding, M.E. Evans and Y. Wang, Magnetostratigraphy of the Baoji loess–paleosol section in the North-Central loess plateau, Quat. Int. 78, 97–102, 1990.
[45] R. Zhu, C. Laj and A. Mazaud, The Matuyama–Brunhes and upper Jaramillo transitions recorded in a loess section at Weinan, north-central China, Earth Planet. Sci. Lett. 125, 143–158, 1994.
[46] J. Imbrie, J.D. Hays, D.G. Martinson, A. McIntyre, A.C. Mix, J.J. Morley, N.G. Pisias, W.L. Prell and N.J. Shackleton, The orbital theory of Pleistocene climate: support from a revised chronology of the marine $\delta^{18}O$ record, in: Milankovitch and Climate, Part 1, A. Berger, ed., pp. 269–305, Reidel, 1984.
[47] D.F. Williams, R.C. Thunell, E. Tappa, D. Rio and I. Raffi, Chronology of the Pleistocene oxygen isotope record: 0–1.8 m.y. B.P., Paleogeogr. Paleoclimat. Paleoecol. 64, 221–240, 1988.
[48] F. Heller, B. Meili, J. Wang, H. Li and T. Liu, Magnetization and sedimentation history of loess in the Central Loess Plateau of China, in: Aspects of Loess Research, T. Liu, ed., pp. 147–163, China Ocean Press, 1987.
[49] L. Tauxe and C. Badgley, Stratigraphy and remanence acquisition of a paleomagnetic reversal in alluvial Siwalik rocks of Pakistan, Sedimentology 35, 697–715, 1988.
[50] K. Verosub, Depositional and postdepositional processes in the magnetization of sediments, Rev. Geophys. Space Phys. 15, 129–143, 1977.
[51] C. Constable and L. Tauxe, Paleointensity in the pelagic realm: marine sediment data compared with archeomagnetic and lake sediment records, Geophys. J. R. Astron. Soc. 90, 43–59, 1987.
[52] B. Singer and M. Pringle, Age and duration of the Matuyama Brunhes geomagnetic polarity reversal from $^{40}Ar/^{39}Ar$ incremental heating analyses of lavas, Earth Planet. Sci. Lett., in press.
[53] M. Sarnthein, H. Erlenkeuser, R. von Grafenstein and C. Schröder, Stable-isotope stratigraphy for the last 750,000 years: "Meteor" core 13519 from the eastern equatorial Atlantic, Meteor Forschungsergeb. C 38, 9–24, 1984.
[54] S.S. Party, Site 851, Proc. ODP Init. Rept. 138, 925, 1991.
[55] J. Chen, J. Farrell, D. Murray and W. Prell, Timescale and paleoceanographic implications of a 3.6 m.y. oxygen isotope record from the northeast Indian Ocean (Ocean Drilling Program Site 758), Paleoceanography 10, 21–47, 1995.
[56] C. Hall and J. Farrell, Laser $^{40}Ar/^{39}Ar$ ages of tephra from Indian Ocean deep-sea sediments: tie points for the astronomical and geomagnetic polarity time scales, Earth Planet. Sci. Lett. 133, 327–338, 1995.
[57] W. Berger, T. Bickert, H. Schmidt, G. Wefer and M. Yasuda, Quaternary oxygen isotope record of pelagic foraminifers: Site 805, Ontong Java Plateau, Proc. ODP Sci. Res. 130, 363–379, 1993.
[58] S.S. Party, Site 805, Proc. ODP Init. Rept. 130, 223–290, 1991.
[59] N. Shackleton and M. Hall, Oxygen and carbon isotope stratigraphy of Deep-Sea Drilling Project Hole 552A: Plio–Pleistocene glacial history, Init. Rept. DSDP 81, 599–609, 1984.
[60] W. Prell, Oxygen and carbon isotope stratigraphies for the Quaternary of Hole 502B: evidence for two modes of isotopic variability, Init. Rept. DSDP 68, 455–464, 1982.
[61] D. Kent and D. Spariosu, Magnetostratigraphy of Caribbean Site 502 hydraulic piston cores, Init. Rept. DSDP 68, 419–433, 1982.
[62] R. Tiedemann, M. Sarnthein and N. Shackleton, Astronomical timescale for the Pliocene Atlantic $\delta^{18}O$ and dust flux records of Ocean Drilling Program site 659, Paleoceanography 9, 619–638, 1994.
[63] L. Tauxe, J. Valet and J. Bloemendal, The magnetostratigraphy of Leg 108 APC Cores, Proc. ODP Sci. Results 108, 865–880, 1989.
[64] B. Linsley and R. Dunbar, The Late Pleistocene history of surface water δ^{13} in the Sulu Sea — possible relationship to Pacific deepwater $\delta^{13}C$ changes, Paleoceanography 9, 317–340, 1994.
[65] D. Schneider, D. Kent and G. Mello, A detailed chronology

of the Australasian impact event, the Brunhes–Matuyama geomagnetic polarity reversal and global climate change, Earth Planet. Sci. Lett. 111, 395–405, 1992.

[66] E. Aksu, A. de Vernai and P. Mudie, High-resolution foraminifer, palynologic and stable isotopic records of upper Pleistocene sediments from the Labrador Sea: paleoclimatic and paleoceanographic trends, Proc. ODP Sci. Results 105, 167–152, 1989.

[67] B. Clement, F. Hall and R. Jarrard, The magnetostratigraphy of ODP Leg 105 sediments, Proc. ODP Sci. Results 105, 583–595, 1989.

[68] S.S. Party, Site 807, Proc. ODP Init. Rept. 130, 369–493, 1991.

[69] I. McDougall, F. Brown, T. Cerling and J. Hillhouse, A reappraisal of the Geomagnetic polarity time scale to 4 Ma using data from the Turkana Basin, East Africa, Geophys. Res. Lett. 19, 2349–2352, 1992.